

Hybrid Deep Neural Network for Classification of Malaria Parasites in Microscopic Images

G. Madhu
Dept. of Information Technology
VNRVJiet
Hyderabad-90, T.S., India
madhu_g@vnrvjiet.in

P. Jogeewara. V.N.S
Dept. of Information Technology
VNRVJiet
Hyderabad-90, T.S., India
jogeewarapuvvala@gmail.com

A. Sai Karthik
Dept. of Information Technology
VNRVJiet
Hyderabad-90, T.S., India
saikarthik.sa@gmail.com

Abstract— Malaria is a critical epidemic disease transmitted by bites from female *Anopheles* mosquitoes, caused by *Plasmodium* parasites. Although it does not spread directly between people, early detection is essential to prevent mild cases from progressing. This research develops a hybrid deep-learning model for classifying malaria parasites in thin blood smears including infected and uninfected erythrocytes. The model employs a convolutional neural network (CNN) with recurrent neural network (RNN) variants. To advance interpretability, the Explainable AI technique, Gradient-weighted Class Activation Map (GradCAM), is incorporated to highlight key regions in the image that support the model's decision-making. Additionally, regularization techniques, including data augmentation, batch normalization, and L2 regularization, are applied to enhance model performance. The proposed CNN-BiGRU model achieved a validation accuracy of 96.7%, precision of 0.97%, recall of 0.96%, F1-score of 0.97%, and an AUC of 0.99 on both training and testing sets.

Keywords— *Bidirectional Gated Recurrent Unit (Bi-GRU), Convolutional Neural Network (CNN), Gated Recurrent Unit (GRU), GradCAM, Malaria parasites, Recurrent Neural Network (RNN).*

I. INTRODUCTION

Malaria is a high-risk disease that causes critical illness, caused by the bites of infected female *Anopheles* mosquitoes. Malaria can be cured and prevented. *Plasmodium falciparum* and *Plasmodium vivax* are the 2 dangerous parasites out of 5 that can cause malaria in humans [1]. According to the World Health Organization (WHO), in 2022, half of the world's population was at risk of malaria, and Africa reports a high rate of malaria cases globally. Some regions of Southeast Asia also report significant malaria cases. Around 249 million cases and 608,000 deaths of malaria will be reported in 2022, and Africa contributes to 94% of the world's malaria cases and 95% of malaria deaths [1]. Counting parasitized cells in thick or thin blood films can diagnose malaria only with human intervention under a microscope [2]. This is indeed one of the frequent methods. However this is a time-consuming process, and the accuracy of the result also depends on inter and intra-observers [2]. To deal with issues regarding long laboratory experiments, automation of this traditional approach leads to early detection of malaria. This gives rise to the use of computerized techniques and hybrid classifiers to develop an automated detection system for malaria [3]. Sophisticated computational procedures are designed for automated medical diagnosis through several medical diagnosis techniques such as MRI, CT scan, ultrasound, and so on, which contribute to faster and more reliable medical diagnosis [4]. The research in [5] has achieved state-of-the-art results using deep neural

networks for image classification. These deep learning architectures outperformed well and provided the best results [6]. Deep neural networks, especially convolutional neural networks (CNN), can potentially automate disease diagnosis, mainly using medical images, providing more accurate and faster methods for disease diagnosis [7]. But, as usual, CNNs lose the proportional spatial relationship between the objects in the image. This limitation can result in misclassification, especially in microscopic images. Thus, developing an accurate and efficient diagnosis system is essential to enhance malaria diagnosis [8]. RNNs are used for sequential data where the information from previous inputs is important [9]. The given inputs are processed sequentially, and to preserve the information from the previous inputs, RNNs store the information in a special state called the hidden state. This makes them suitable for time series prediction tasks, text and speech analysis, and anywhere temporal or sequential data is a major factor [9]. Bidirectional Gated Recurrent Units (BiGRU) are introduced to improve the Gated Recurrent Unit (GRU) architecture (which are variants of RNN) and contain bidirectional processing. BiGRU read through the sequence data twice, from left to right and right to left, thereby giving the network context information [10]. The given bidirectional strategy can show better results in cases where it is important to predict the next and previous context of the sequence, such as speech recognition and text classification [10]. Deep neural networks, especially CNNs, are widespread in medical analysis. However, understanding the decision-making of CNNs is still challenging, and there is a need for explaining the decisions. This motivated researchers to develop explainable AI techniques. Ramprasaath R. Selvaraju et al. [11] presented the visual explanation procedure with gradient-weighted class activation mapping (Grad-CAM) to advance the explainability and transparency of CNNs. Grad-CAM highlights the relevant areas of an image that contribute most to the model's classification decision by utilizing the gradients of the target concept from the final convolutional layer to produce class-discriminative heatmaps. To develop malaria detection and classification, a more effective and precise diagnostic model must be established. This study presents an automated diagnostic model for the detection and classification of parasites associated with malaria in blood cell images.

- To extract the spatial features and temporal features using CNN and RNN.
- Integration of CNN with variants of RNNs, particularly GRU and BiGRU, to emphasize both spatial feature extraction and sequence context understanding.
- To incorporate Grad-CAM visualizations to make the research more understandable and transparent.

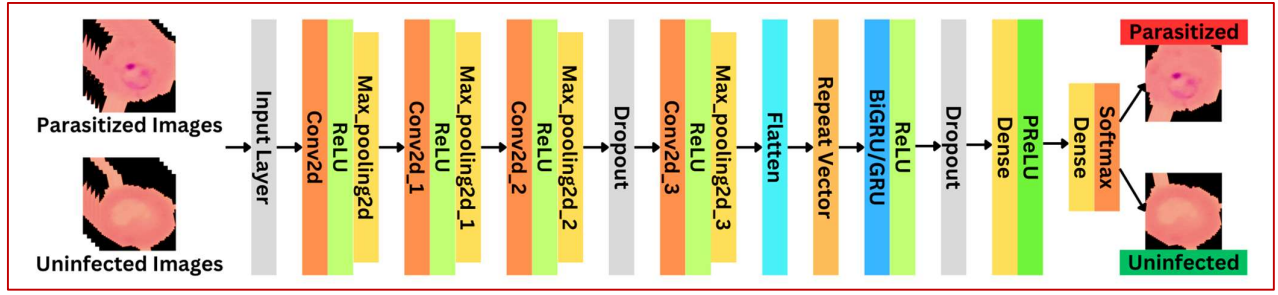


Fig. 1. The Architecture of proposed CNN-BiGRU and CNN-GRU Models

TABLE I. DESCRIBES THE DISTRIBUTION OF MALARIA DATA SAMPLES INTO VARIOUS TRAINING AND TESTING SPLITS

Dataset Split	Training Data	Testing Data
90-10	24802	2756
80-20	22046	5512
70-30	19290	8268
60-40	16534	11024
50-50	13779	13779
40-60	11023	16535
30-20	8267	19291
20-80	5511	22047
10-90	2755	24803

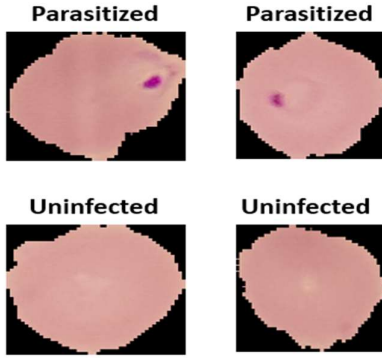


Fig. 2. Sample images of Malaria Parasitized and Uninfected Cell Images

II. PREVIOUS WORKS

A. Dev et al., [12] proposed a hybrid deep learning network that combines the strengths of different deep learning networks to improve the accuracy of malaria detection using microscopic blood smears. The authors developed several hybrid networks by combining CNN and variants of RNN, i.e., GRU, LSTM, and BiLSTM. The model proposed by the authors, the CNN-LSTM-BiLSTM model, achieved the highest accuracy of 96.2%. R. Z. Lekeufack Fouleack et al. [13] employed CNN for malaria detection and achieved an accuracy of 96.66%. The authors incorporated Grad-CAM to explain the results. A. Dev et al., [14] proposed the use of hybrid deep learning models for malaria parasite detection and three hybrid models by combining CNN with LSTM, BiLSTM, and GRU. The model proposed by the authors, the CNN-GRU hybrid model, achieved the highest accuracy of 96.01%, the lowest type-1 error rate of 1.81%, and the lowest type-2 error rate of 2.18%. Md. Robiul et al. [15] proposed an advanced approach for malaria detection using transformer architecture integrated with Grad-CAM and achieved an

accuracy of 96.41% for the original dataset. Imen Jdey et al., [16] demonstrated the role of machine learning and deep learning in the detection of malaria. They showcased some ML and DL example algorithms, and the problem areas related to them and recommended some techniques, such as data augmentation, transfer learning, etc., in the future to fine-tune the model. Alsanousi WA et al., [17] developed a novel deep-learning hybrid network to classify the mitochondrial proteins of the Plasmodium falciparum parasite, which is responsible for malaria in humans. The authors proposed a novel hybrid network by combining a 1D CNN and a BiGRU unit for classification and achieved 90.96% accuracy on the PF4204 dataset and 98.57% accuracy on the PF2095 dataset. Marques et al., [18] proposed a support decision system for malaria parasites detection based on CNN. The model proposed by the authors is based on the EfficientNetB0 architecture and evaluated with 10-fold cross-validation, achieving 97.74% precision, 98.82% recall, 98.28% F1-Score, and a 99.76% ROC value. Aayush Kumar et al. [19] proposed MOSQUITO-NET for malaria detection using CNNs and Grad-CAM to explain the decision of the model and achieved an accuracy of 95%. M. K. Gourisaria et al., [20] developed a deep CNN-based deep learning network for malaria parasite detection, and the accuracy achieved by the proposed model was 95.23%. D. Shah et al., [21] discussed the importance of early and accurate diagnosis of malaria and developing an automated system for malaria diagnosis using deep learning. The model proposed by the authors is based on CNN and achieved an accuracy of 95% even with limited computational resources. A. S. B. Reddy and D. S. Juliet [22] focused on the applicability of transfer learning for malaria detection, and as a result, they have seen that transfer learning works well in the detection of malaria. The authors employed the pre-trained model ResNet-50, which is a deep CNN network, to detect malaria and were able to get a training accuracy of 95.91% while the validation accuracy stood at 95.4%. S. N. Dharpal and D. A. V. Malviya [23] focused on developing an automated system for malaria parasite detection using SVM classifiers. The model proposed by the authors achieved 97.02% accuracy. Razzak et al., [24] described the various challenges in the medical department and discussed how deep learning helped in refining several specialties, such as medical image analysis through image segmentations and image classifications. J.A. Quinn et al., [25] added to the problem of the identification of infectious diseases in conditions where there are limited laboratory facilities and highly qualified technicians by proposing a deep CNN and evaluating the model on three different microscopic tasks.

TABLE II. TRAINING AND TESTING TIME COMPARISON OF BiGRU AND GRU NETWORKS USING DIFFERENT OPTIMIZERS, REGULARIZATION TECHNIQUES, AND DATA AUGMENTATION

Network		BiGRU				GRU			
		Training Time(s)		Testing Time(s)		Training Time(s)		Testing Time(s)	
		Adam	Nadam	Adam	Nadam	Adam	Nadam	Adam	Nadam
Data Augmentation	L2	2283.17	3155.90	1.15	1.09	1562.97	2156.71	0.97	0.98
	No L2	1896.15	2429.49	1.08	0.99	1492.91	2613.33	0.85	2.09
No Data Augmentation	L2	1289.35	1409.44	0.96	0.99	1147.76	1237.75	0.67	1.03
	No L2	1288.43	1363.92	0.95	1.04	1202.19	1288.21	0.66	0.98

TABLE III. EVALUATION METRICS COMPARISON FOR GRU AND BiGRU NETWORKS USING DIFFERENT OPTIMIZERS, REGULARIZATION TECHNIQUES, AND DATA AUGMENTATION

Evaluation Metrics	Optimizer	Data Augmentation				No Data Augmentation			
		GRU		BiGRU		GRU		BiGRU	
		L2	No L2	L2	No L2	L2	No L2	L2	No L2
Training Accuracy	Adam	95.1	99.1	95.0	99.2	95.9	49.6	95.9	99.1
	Nadam	95.1	99.0	95.1	99.1	96.1	99.0	95.9	98.9
Validation Accuracy	Adam	94.7	94.6	95.2	94.5	95.7	50.0	95.7	95.9
	Nadam	95.4	94.4	94.8	94.8	95.8	94.9	96.7	96.0
Precision	Adam	0.97	0.95	0.96	0.96	0.97	0.50	0.96	0.97
	Nadam	0.97	0.95	0.96	0.96	0.97	0.97	0.97	0.96
Recall	Adam	0.92	0.94	0.94	0.94	0.94	1.00	0.95	0.95
	Nadam	0.94	0.94	0.94	0.93	0.94	0.93	0.96	0.96
F1-Score	Adam	0.95	0.95	0.95	0.95	0.96	0.67	0.96	0.96
	Nadam	0.95	0.94	0.95	0.95	0.96	0.95	0.97	0.96
AUC-Training Set	Adam	0.98	0.99	0.98	0.99	0.99	0.5	0.99	0.99
	Nadam	0.98	0.99	0.98	0.99	0.99	0.99	0.99	0.99
AUC-Testing Set	Adam	0.98	0.97	0.98	0.97	0.98	0.5	0.98	0.98
	Nadam	0.98	0.97	0.98	0.98	0.98	0.97	0.99	0.98

TABLE IV. TRAINING AND TESTING TIME COMPARISON OF GRU AND BiGRU NETWORKS WITH A VARIETY OF TRAIN-TEST SPLITS

Dataset Split	Training Time(s)		Testing Time(s)	
	BiGRU	GRU	BiGRU	GRU
90-10	1409.44	1228.26	0.99	0.95
80-20	1240.62	1167.28	2.06	1.74
70-30	1264.79	1104.05	2.48	2.37
60-40	1008.89	987.15	2.94	4.10
50-50	923.60	866.15	4.51	3.91
40-60	872.32	808.93	5.38	4.73
30-70	747.27	685.70	5.71	8.63
20-80	566.49	567.71	6.40	7.66
10-90	450.66	446.45	9.21	6.81

III. METHODOLOGY

A. Dataset Description

The dataset comprises two categories of thin blood smear images of erythrocytes: Parasitized and Uninfected. This research utilizes the publicly available Malaria Cell Images Dataset from Kaggle [26]. The dataset is organized into two folders: Infected (Parasitized) and Uninfected, each containing 13,779 color images of erythrocytes, resulting in a total of 27,558 color images. To standardize image dimensions, all images were resized to 128x128 pixels while maintaining the original three color channels (RGB). Fig. 2 presents sample images of both Parasitized and Uninfected Malaria Cell Images.

B. CNN-GRU and CNN-BiGRU

The present study focuses on assessing the efficiency of CNN-GRU and CNN-BiGRU models accompanied by two optimizers: Nadam and Adam. Fig.1. Describe the architecture of the present study. The architecture of the model entails several convolutional layers, a GRU/BiGRU layer, and dense layers. Looking at the CNN part of the model, the first layer is the Conv2D layer with a 2 x 2 filter size, 32 filters, and ReLU activation, taking input of the shape

128x128x3. This is then followed by the MaxPooling2D layer, which is used to reduce the size of output along the space dimension but retains the volume size. The pattern continues with another Conv2D layer, this one with 32 filters, followed by another MaxPooling2D layer. Next, two Conv2D layers with 64 filters are added; each is accompanied by the MaxPooling2D operation. A dropout layer with a 50% dropout rate was added to prevent overfitting after the second Conv2D layer with 64 filters. Next, a Flatten Layer and Repeat Vector are added. Next, a GRU layer is added. Finally, the model includes a dropout layer and two dense layers: the first dense block was equipped with 512 filters and a parametric ReLU activation function, whereas the second has 2 filters and uses SoftMax activation. The model was trained with a Nadam optimizer, sparse categorical cross-entropy loss function, and accuracy metric. The image size was constant at 128 while the batch size was set to 64 for the experiment. However, the learning curves pointed out that, as epochs increase, the training as well as the validation start to increase and are not consistent.

The CNN part of the model remained the same as before, we replaced the GRU layer with a bidirectional GRU layer with 64 units and trained with the same two optimizers. The two optimizers had similar training and test accuracies; however, the resulting models were highly overfitted. The Adam optimizer was marginally better, with less test loss and shorter training time. Nevertheless, it is also observed that the model is overfitting; more regularization techniques or data augmentation must be applied. These observations stress the necessity of the application of other approaches to prevent the overfitting issue and improve stability. The findings of this architecture are presented in Table II and Table III.

TABLE V. EVALUATION METRICS COMPARISON OF CNN-GRU NETWORK WITHOUT DATA AUGMENTATION AND WITH L2 REGULARIZATION

Evaluation Metrics	Generalization								
	Train-Test Splits								
	90-10	80-20	70-30	60-40	50-50	40-60	30-70	20-80	10-90
Training Accuracy	95.9	96.0	95.7	96.0	96.1	96.4	96.7	97.4	97.9
Validation Accuracy	95.8	96.2	96.1	95.9	95.2	95.5	94.7	94.5	95.2
Precision	0.97	0.97	0.97	0.97	0.97	0.96	0.97	0.97	0.97
Recall	0.95	0.95	0.95	0.95	0.93	0.95	0.93	0.92	0.93
F1-Score	0.96	0.96	0.96	0.96	0.95	0.96	0.95	0.94	0.95
AUC-Training Set	0.99	0.99	0.99	0.99	0.99	0.99	0.99	0.99	0.99
AUC-Testing Set	0.98	0.98	0.98	0.98	0.98	0.98	0.98	0.98	0.97

^a Observation: The 80-20 split performed best compared to other models with 96.0% accuracy and 96.2% validation accuracy.

TABLE VI. EVALUATION METRICS COMPARISON OF CNN-BiGRU NETWORK WITHOUT DATA AUGMENTATION AND WITH L2 REGULARIZATION

Evaluation Metrics	Generalization								
	Train-Test Splits								
	90-10	80-20	70-30	60-40	50-50	40-60	30-70	20-80	10-90
Training Accuracy	95.9	95.9	95.8	95.9	96.0	96.1	96.6	96.8	98.1
Validation Accuracy	96.7	96.1	95.7	96.0	95.9	95.9	95.6	95.5	94.8
Precision	0.97	0.97	0.96	0.96	0.97	0.97	0.97	0.96	0.97
Recall	0.96	0.95	0.96	0.96	0.95	0.95	0.94	0.95	0.92
F1-Score	0.97	0.96	0.96	0.96	0.96	0.96	0.95	0.95	0.95
AUC-Training Set	0.99	0.99	0.99	0.99	0.99	0.99	0.99	0.99	0.99
AUC-Testing Set	0.99	0.98	0.98	0.98	0.98	0.98	0.98	0.98	0.97

^b Observation: The 90-10 split performed best compared to other models with 95.9% accuracy and 96.7% validation accuracy.

C. Regularization Techniques

R. Moradi et al., [27] provided a comprehensive survey of the Methods to reduce the model complexity that is crucial in machine learning and deep learning to overcome the issue of overfitting and generating good results on new data. Hinton G et al., [28] introduced a technique called "Dropout". This cool technique randomly "freezes" a part of neurons during the training of a neural network. In other words, during each training epoch, some of the neurons and their interconnections are partially or fully 'removed' from the network [28]. This makes sure that the neurons are not completely dependent on the other ones. Iofe S et al., [29] introduced "Batch Normalization", a technique for improving deep neural network training. This method scales down the final layer of the previous activation by subtracting the mean from it and dividing it by the standard deviation of a batch. After that, the values in the vector are scaled and shifted according to the learned parameters [29]. This prevents the model from learning specific features of the training data and makes it easy for the model to predict unseen data. An optimizer [30], specifically a learning rate schedule (schedule lr), is an essential aspect of the optimization of deep learning models. It refers to the practice of changing the learning rate while training by some schedule as opposed to keeping it fixed. This method helps make more rapid convergence and prevents the model from sticking to local optima as it boosts the performance of the model [30]. Data augmentation is a technique to create new training samples by applying various transformations to the original data. We can do things like rotating, translating, flipping, and changing the colors of the data [31]. Each of these regularization techniques plays a crucial role in improving the generalization capabilities of ML and DL models. By using these methods, models are less likely to overfit and more likely to perform well on real-world data [32]. So, by employing these techniques, we're optimizing the model to be more flexible and accurate in handling new and unseen data.

D. Regularized Architectures

We proceeded with the same model that is mentioned as CNN-GRU and CNN-BiGRU architectures. This time we added L2 regularization, but data augmentation was not applied. The L2 regularization method is useful in penalizing large weights, hence eliminating overfitting. In the Next phase of our research, we increased the baseline model's robustness by the inclusion of data augmentation into the baseline model as well as L2 regularization. The augmentations have doubled the images, making the training samples more varied and probably reducing overfitting. The model's architecture remained the same with convolutional layers, a GRU layer, and dense layers. In the Next phase, the model is trained with data augmentation but without L2 regularization. The findings are presented in Table II and Table III. Model Without Data Augmentation and with L2 Regularization performed best compared to other proposed architecture, CNN-GRU with a Training Accuracy of 96.1% and Validation Accuracy of 95.8% with Nadam Optimizer and CNN-BiGRU with a Training Accuracy of 95.9% and Validation Accuracy of 96.7%. Without Data Augmentation and with L2 Regularization Architecture is selected as the best architecture for further Training experiments.

IV. RESULTS

Both GRU and BiGRU architectures Without Data Augmentation and with L2 Regularization performed best with the Nadam optimizer. Without Data Augmentation and with L2 Regularization Architecture is selected as the best architecture for further training experiments. We will test this architecture with a variety of train-test splits to show generalization across data distributions. Table I describes the distribution of malaria data samples into various training and testing splits. Testing across these train-test splits will enable Us to show how well the model generalizes on new data and performs concerning different quantities of training data.

TABLE VII. DESCRIBES LEARNING CURVES, ROC CURVE, AND CONFUSION MATRIX OF GRU NETWORK WITH A VARIETY OF TRAIN-TEST SPLITS

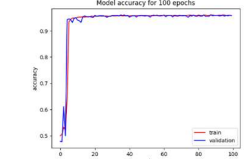
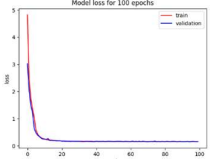
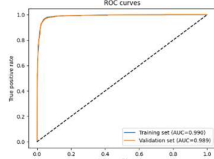
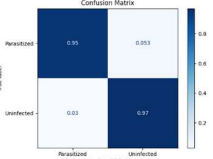
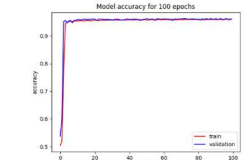
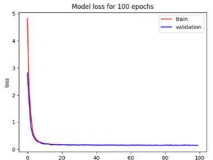
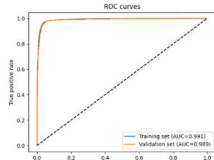
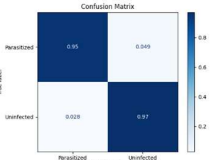
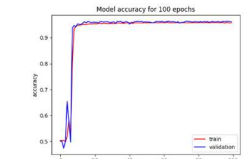
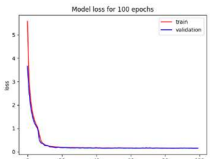
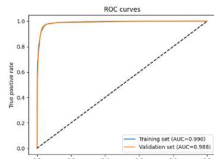
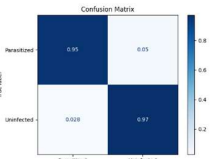
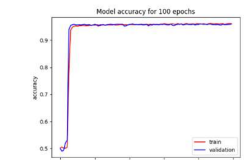
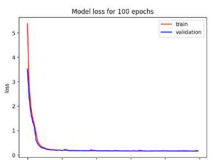
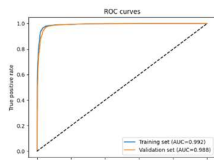
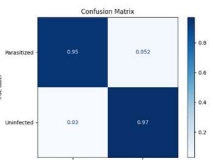
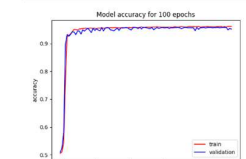
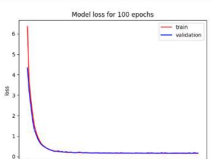
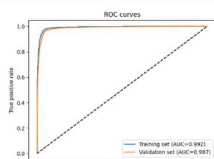
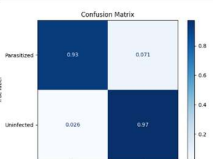
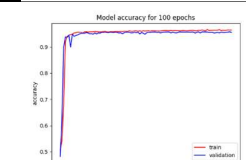
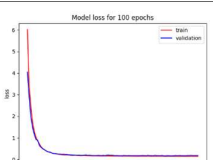
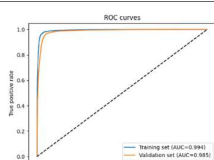
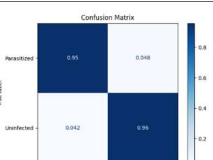
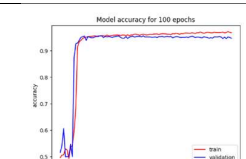
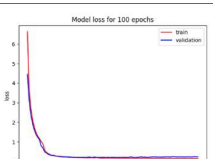
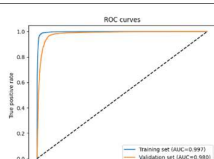
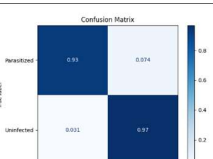
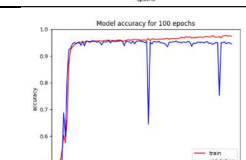
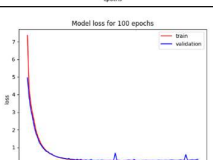
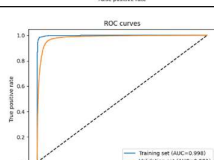
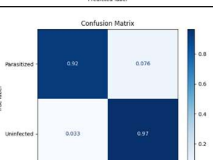
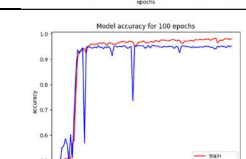
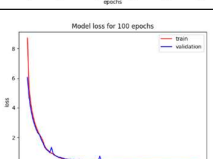
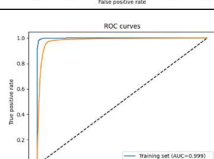
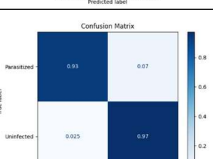
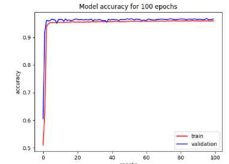
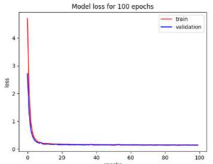
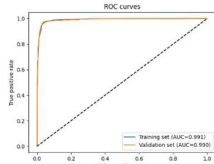
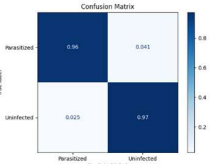
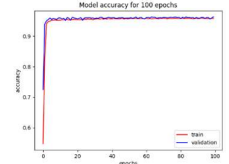
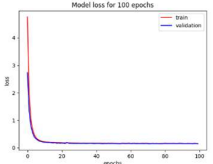
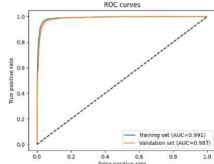
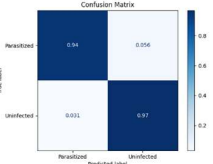
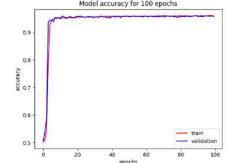
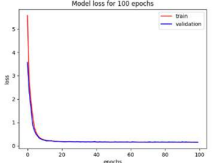
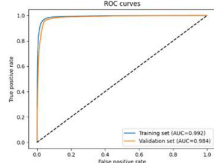
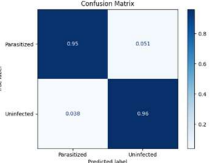
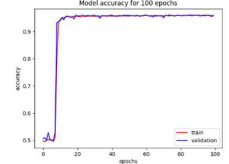
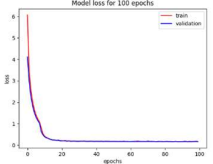
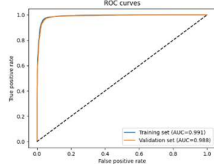
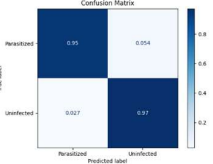
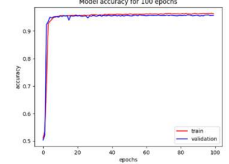
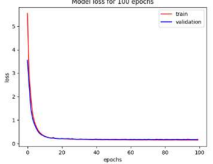
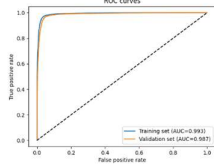
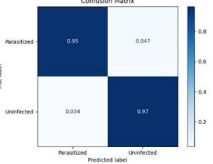
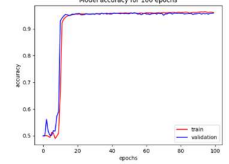
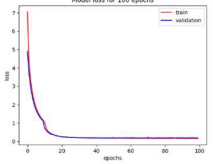
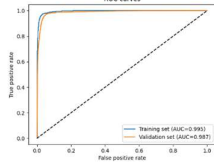
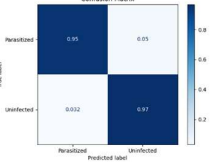
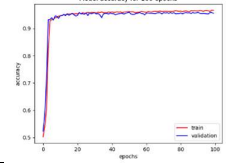
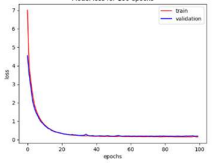
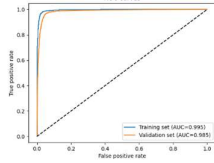
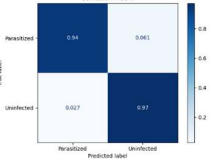
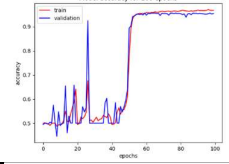
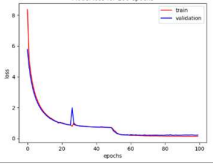
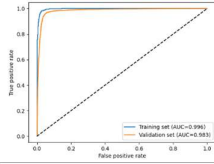
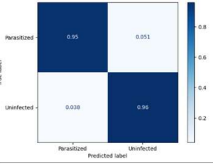
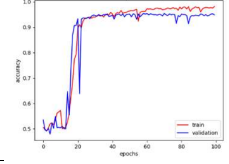
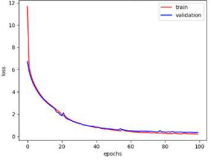
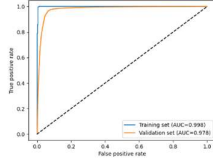
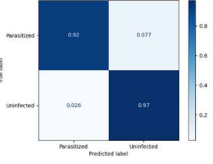
Accuracy Plot	Loss Plot	Split	ROC Curve	Confusion Matrix
		90-10		
		80-20		
		70-30		
		60-40		
		50-50		
		40-60		
		30-70		
		20-80		
		10-90		

TABLE VIII. DESCRIBES LEARNING CURVES, ROC CURVE, AND CONFUSION MATRIX OF BIGRU NETWORK WITH A VARIETY OF TRAIN-TEST SPLITS

Accuracy Plot	Loss Plot	Split	ROC Curve	Confusion Matrix
		90-10		
		80-20		
		70-30		
		60-40		
		50-50		
		40-60		
		30-70		
		20-80		
		10-90		

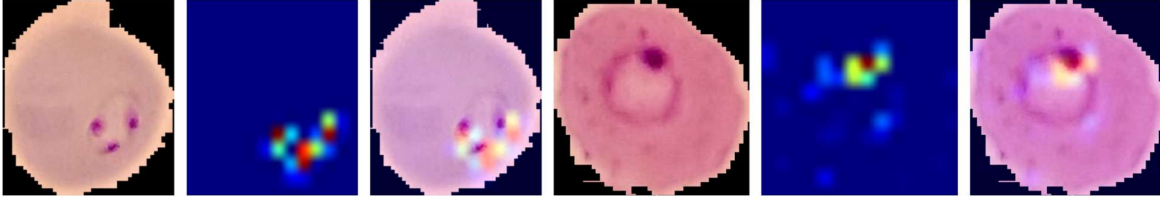


Fig. 3. GradCAMs generated by CNN-GRU model for Parasitized Images.

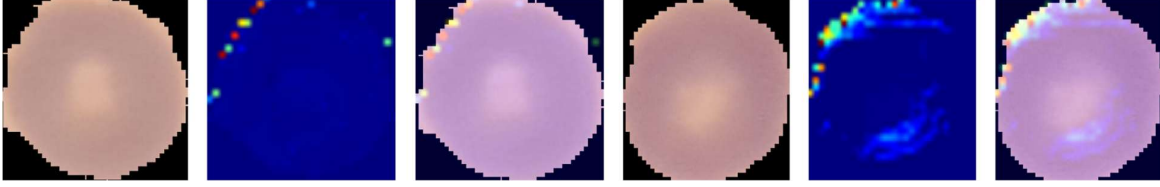


Fig. 4. GradCAMs generated by CNN-GRU model for Uninfected Images.

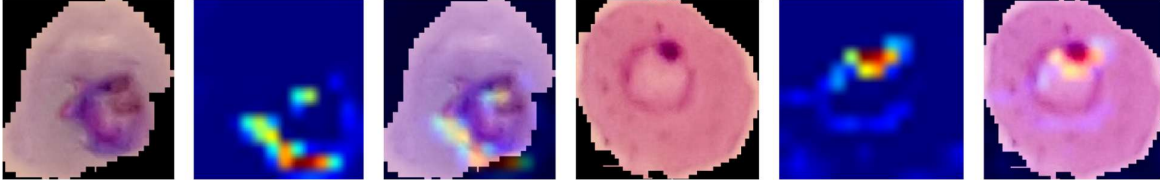


Fig. 5. GradCAMs generated by CNN-BiGRU model for Parasitized Images.

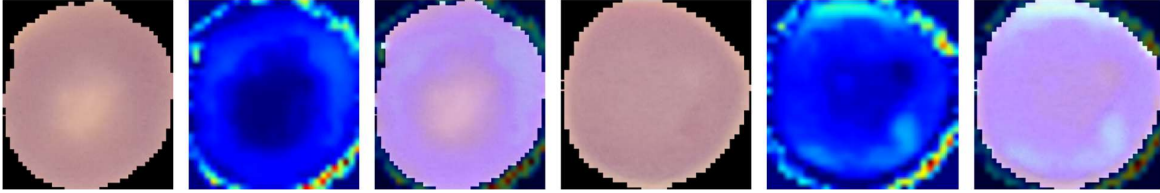


Fig. 6. GradCAMs generated by CNN-BiGRU model for Uninfected Images.

The findings are presented in Table IV, Table V, Table VI, Table VII, and Table VIII. An 80-20 split of the CNN-GRU network achieved the highest validation accuracy of 96.2%, while a 90-10 split of the CNN-BiGRU network achieved the highest validation accuracy of 96.7%. The GradCAM visualizations generated by these models are shown in Fig. 3, Fig. 4, Fig. 5, and Fig. 6. The analysis of GradCAM is mentioned below:

Initially, an input image is passed through the CNN to obtain the output predictions and the activations of the last CNN layer in which most of the analysis happens are stored. Then, the gradients of the score for the class C_i , i.e. S^{C_i} , concerning the feature maps f^k of the last CNN layer are computed i.e. $\frac{\partial S^{C_i}}{\partial f^k}$ Using backpropagation. Then the importance weights of each feature map k , i.e. $N_k^{C_i}$ are calculated by globally averaging the obtained gradients across the dimensions, i.e. height h and width w Of each feature map as described in (1).

$$N_k^{C_i} = \frac{1}{Z} \sum_h \sum_w \frac{\partial S^{C_i}}{\partial f^k} - (1)$$

Where Z There are no. of pixels in the feature map.

The weighted combination of feature maps is computed using weights obtained by (1) and followed by *ReLU* Activation as described in (2), which represents the important regions of the feature map k for the target class C_i .

$$HeatMap = ReLU(\sum_k N_k^{C_i} f^k) - (2)$$

Thus, the heat map generated by (2) is up-sampled to match the dimensions of the input image. The generated heat map can be overlaid on the input image to provide a visual interpretation of which regions of the image are influencing most on the model's decision.

CNN-BiGRU Network without Data Augmentation and With L2 Regularization Outperforms other trained models with the highest Validation Accuracy of 96.7% and 95.9% Training Accuracy, with training and testing time 1409 and 0.99 seconds respectively. 0.97 Precision, 0.96 Recall, 0.97 F1-Score, 0.99 AUC Training Set and 0.99 AUC Testing Set.

A. Imbalanced Dataset Implementation Results

The most efficient and high-accuracy models which are CNN-GRU and CNN-BiGRU without data augmentation and regularization are implemented using an imbalanced dataset that uses 40% of the original parasitized and 70% of the original uninfected dataset. The testing accuracy of CNN-GRU is 95.6% and CNN-BiGRU is 95.58% which is almost equal to the balanced dataset results and the confusion matrix shown in Fig.7 and Fig.8.

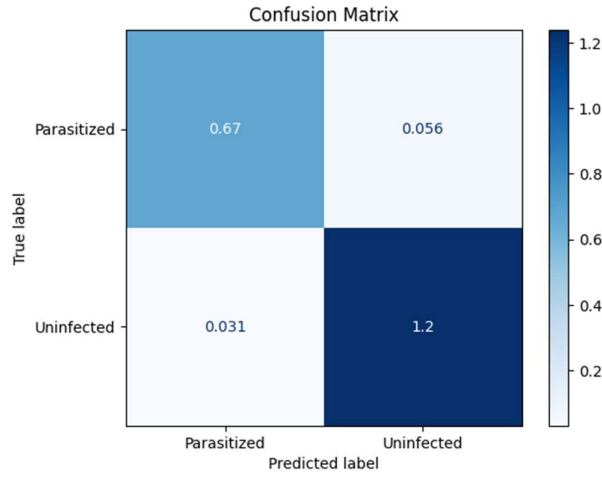


Fig. 7. Confusion Matrix of CNN-GRU model for Imbalanced dataset.

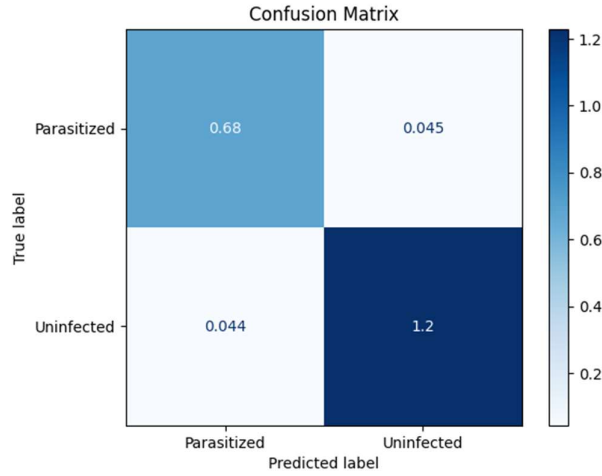


Fig. 8. Confusion Matrix of CNN-BiGRU model for Imbalanced dataset

V. CONCLUSION

This study introduced a hybrid deep-learning model for classifying malaria parasites in microscopic images. Experiment results showed that the proposed model can significantly enhance malaria detection in thin blood smears. The proposed model integrates CNN with RNN variants (GRU and BiGRU) and outperforms both traditional laboratory techniques and existing methods. Further, overfitting was addressed using multiple techniques that boosted model performance. However, GradCAM was applied to increase model transparency, offering visual interpretations of predictions, and aiding the decision-making process. The model achieved a validation accuracy of 96.7%, training accuracy of 95.9%, precision of 0.97, recall of 0.96, F1-score of 0.97, and an AUC of 0.99 respectively. These results suggest that the proposed CNN-RNN architecture is highly effective for malaria parasite detection. Future research may focus on deploying the model for interactive, real-time applications and expanding its functionality to detect other parasitic diseases, making it even more beneficial for diagnostic purposes which will be used to identify parasite species and stages in thin blood smears.

TABLE IX. COMPARISON OF THE PROPOSED MODEL WITH EXISTING MODELS

Authors	Approach	Accuracy (%)
Praneesh, Dr et al., (2024) [33]	CNN	94.99
D. Shah et al., (2020) [16]	CNN	95
Aayush Kumar et al., (2020) [24]	CNN + GradCAM	95
M. K. Gourisaria et al., (2020) [15]	CNN	95.23
A. S. B. Reddy and D. S. Juliet (2019) [18]	ResNet-50	95.4
A. Dev et al., (2023) [22]	CNN-GRU-GRU	96.01
M. M. Fouda et al., (2024) [20]	CNN-LSTM-BiLSTM	96.2
Md. Robiul et al., (2022) [23]	Multiheaded Attention-based Transformer + GradCAM	96.41
R. Z. Lekeufack Foulefack et al., (2024) [25]	CNN + GradCAM	96.66
Proposed Model	CNN + BiGRU + GradCAM	96.7

REFERENCES

- [1] https://www.who.int/health-topics/malaria#tab=tab_1
- [2] M.J. Cuomo, B. N Lawrence and D. B. White, "Diagnosing medical parasites: a public health officers guide to assisting laboratory and medical officers," Air Education and Training Command Randolph AFB TX, 2009.
- [3] Devi, S.S., Roy, A., Singha, J. et al. Malaria-infected erythrocyte classification based on a hybrid classifier using microscopic images of thin blood smear. *Multimed Tools Appl* 77, 631–660 (2018). <https://doi.org/10.1007/s11042-016-4264-7>
- [4] Rajaraman S, Jaeger S, Antani SK. Performance evaluation of deep neural ensembles toward malaria parasite detection in thin-blood smear images. *PeerJ*. 2019 May 28;7:e6977. doi: 10.7717/peerj.6977. PMID: 31179181; PMCID: PMC6544011.
- [5] A. Krizhevsky, S. Ilya Sutskever and E. H. Geoffrey, "ImageNet classification with deep convolutional neural networks," *Communications of the ACM*, vol. 60, no. 6, pp. 84-90, 2017.
- [6] K. He, X. Zhang, S. Ren, J. Sun, Delving deep into rectifiers: surpassing human-level performance on ImageNet classification, in: *Proceedings of the IEEE International Conference on Computer Vision*, 2015, pp. 1026–1034.
- [7] M.I. Razzak, SaeedaNaz and A. Zaib. "Deep learning for medical image processing: Overview, challenges, and the future," *Classification in BioApps*. Springer, Cham, pp. 323-350, 2018.
- [8] N. Tajbakhsh, J.Y. Shin, S.R. Gurudu, R.T. Hurst, C.B. Kendall, M.B. Gotway, and J. Liang, 'Convolutional Neural Networks for Medical Image Analysis: Fine Tuning or Full Training?', *IEEE Transactions on Medical Imaging*, vol. 35, no. 5, pp. 1299-1312, 2016.
- [9] I. Sutskever, O. Vinyals, and Q.V. Le, Sequence to Sequence Learning with Neural Networks', *Advances in Neural Information Processing Systems (NIPS)*, vol. 27, pp. 3104-3112, 2014.
- [10] C. Tang, D. Zhang, and Q. Tian, 'Convolutional Neural Network–Bidirectional Gated Recurrent Unit Facial Expression Recognition Method Fused with Attention Mechanism', *Applied Sciences*, vol. 13, no. 22, pp. 12418, Nov. 2023, doi:10.3390/app132212418.
- [11] Ramprasaath R. Selvaraju, Michael Cogswell, Abhishek Das, Ramakrishna Vedantam, Devi Parikh, Dhruv Batra, "Grad-CAM: Visual Explanations from Deep Neural Networks via Gradient-based Localization", preprint arXiv:1610.02391

- [12] A. Dev, M. M. Fouda, L. Kerby and Z. Md Fadlullah, "Advancing Malaria Identification From Microscopic Blood Smears Using Hybrid Deep Learning Frameworks," in *IEEE Access*, vol. 12, pp. 71705-71715, 2024, doi: 10.1109/ACCESS.2024.3402442.
- [13] R. Z. Lekeufack Foulefack, A. A. Akinyelu, D. Ranirina and B. N. Mpinda, "Malaria Parasite Detection in Microscopic Blood Smear Images Using Deep Learning Techniques," 2024 International Joint Conference on Neural Networks (IJCNN), Yokohama, Japan, 2024, pp. 1-8, doi: 10.1109/IJCNN60899.2024.10651385.
- [14] A. Dev, M. M. Fouda, L. Kerby and Z. M. Fadlullah, "On Improving Malaria Parasite Detection from Microscopic Images: A Comparative Analytics of Hybrid Deep Learning Models," 2023 11th International Conference on Information and Communication Technology (ICoICT), Melaka, Malaysia, 2023, pp. 417-422, doi: 10.1109/ICoICT58202.2023.10262467.
- [15] Md. Robiul, Md. Nahiduzzaman, Md. Omar Faruq Goni, Abu Sayeed, Md. Shamim Anower, Mominul Ahsan, and Julfikar Haider. 2022. "Explainable Transformer-Based Deep Learning Model for the Detection of Malaria Parasites from Blood Cell Images" *Sensors* 22, no. 12: 4358. <https://doi.org/10.3390/s22124358>
- [16] Imen Jdey, Ghazala Hcini, Hela Ltifi, 2022. Deep learning and machine learning for Malaria detection: overview, challenges, and future directions. *Arxiv preprint arXiv:2209.13292*
- [17] Alsanousi WA, Ahmed NY, Hamid EM, Elbashir MK, Musa MEM, Wang J, Khan N, Afnan. A novel deep learning-assisted hybrid network for plasmodium falciparum parasite mitochondrial proteins classification. *PLoS One*. 2022 Oct 6;17(10):e0275195. doi: 10.1371/journal.pone.0275195. PMID: 36201724; PMCID: PMC9536844.
- [18] Marques, Gonalo, Antonio Ferreras, and Isabel de la Torre-Diez. "An ensemble-based approach for automated medical diagnosis of malaria using EfficientNet." *Multimedia tools and applications* 81.19 (2022): 28061-28078.
- [19] Aayush Kumar, Sanat B Singh, Suresh Chandra Satapathy, Minakhi Rout, "MOSQUITO-NET: A deep learning based CADx system for malaria diagnosis along with model interpretation using GradCam and class activation maps" *arxiv preprint arXiv:2006.10547*
- [20] M. K. Gourisaria, S. Das, R. Sharma, S. S. Rautaray, and M. Pandey, "A deep learning model for malaria disease detection and analysis using deep convolutional neural networks," *Int. J. Emerg. Technol.*, vol. 11, no. 2, pp. 699–704, 2020
- [21] D. Shah, K. Kawale, M. Shah, S. Randive and R. Mapari, "Malaria Parasite Detection Using Deep Learning : (Beneficial to humankind)," 2020 4th International Conference on Intelligent Computing and Control Systems (ICICCS), Madurai, India, 2020, pp. 984-988, doi: 10.1109/ICICCS48265.2020.9121073.
- [22] A. S. B. Reddy and D. S. Juliet, "Transfer learning with ResNet-50 for malaria cell-image classification," in *Proc. Int. Conf. Commun. Signal Process. (ICCSPP)*, Apr. 2019, pp. 0945–0949
- [23] S. N. Dharpal and D. A. V. Malviya, "Automated enumeration of malaria parasite using SVM classifier," *Int. J. Res. Trends Innov.*, vol. 3, no. 10, pp. 159–165, 2018.
- [24] Razzak, M. I., Naz, S., & Zaib, A. Deep learning for medical image processing: Overview, challenges, and the future. *Classification in BioApps: Automation of decision making*, 323-350, 2018.
- [25] J.A. Quinn, R. Nakasi, P.K.B. Mugagga, P. Byanyima, W. Lubega, A. Andama, Deep convolutional neural networks for microscopy-based point of care diagnostics, in *Machine Learning for Healthcare Conference*, 2016, pp. 271–281.
- [26] R. Moradi, R. Berangi, and B. Minaei, "A survey of regularization strategies for deep models," *Artificial Intelligence Review*, vol. 53, no. 6, pp. 3947–3986, 2020.
- [27] <https://www.kaggle.com/datasets/iarunava/cell-images-for-detecting-malaria>
- [28] Hinton G, Srivastava N, Krizhevsky A, Sutskever I, Salakhutdinov R (2012c) Improving neural networks by preventing co-adaptation of feature detectors, *arXiv preprint arXiv:1207.0580*
- [29] Iofe S, Szegedy C (2015) Batch normalization: accelerating deep network training by reducing internal covariate shift. *arXiv:1502.03167*
- [30] Goodfellow I, Bengio Y, Courville A (2016) *Deep learning*. MIT Press, Cambridge.
- [31] Luke Taylor, Geoff Nitschke, Improving Deep Learning using Generic Data Augmentation *arxiv preprint arXiv:1708.06020*
- [32] C. F. G. Dos Santos and J. P. Papa, "Avoiding overfitting: A survey on regularization methods for convolutional neural networks," *ACM Computing Surveys (CSUR)*, vol. 54, no. 10s, pp. 1–25, 2022.
- [33] Praneesh, Dr & K, Sai & N, Febina & Ashwanth. V., (2024). Malaria Parasite Detection in Microscopic Blood Smear Images Using Deep Learning Approach. *International Journal of Scientific Research in Computer Science, Engineering and Information Technology*. 10. 669-676. 10.32628/CSEIT2410286.